

Moment inequalities and high-energy tails for electron distribution function of the Boltzmann transport equation in semiconductors.

Orazio Muscato

Dipartimento di Matematica e Informatica
Università di Catania
Viale Andrea Doria 6 - 95125 Catania, Italy

e-mail: *muscato@dmf.unict.it*

Abstract

In this paper we prove the existence of the high-energy tails for electron distribution function of the Boltzmann equation for semiconductors, in the stationary and homogeneous regime, in the analytic band approximation and scattering with acoustic and optical phonons and impurities. We also prove numerically that the tail is a global maxwellian in the parabolic band approximation, and in the quasi parabolic band case, a power law of the global maxwellian.

keywords Boltzmann-Poisson system for semiconductors, Monte Carlo Method, Semiconductors.

MSC classifications 76P05, 65C05, 82B35,

1 Introduction

In recent years, the dimensions of MOS devices have been scaled down reaching sub-micrometric order. As a result, large electric fields near the drain region generate hot or energetic electrons. Hot electrons can heat the device with important consequences for long-term reliability, or can be injected into the oxide creating an instability in the device performance. Moreover, injection of hot electron onto a floating gate has been widely used as the writing mechanism in EPROM and flash EEPROM device. To model these effects is a difficult task, because they depend upon the small fraction of carriers with energy above certain thresholds and hence the knowledge of the tail of the electron energy distribution (hereafter EED) is required.

The natural framework for describing these regimes is the Boltzmann Transport Equation (BTE) with the adequate scattering mechanisms, coupled with the Poisson equation. To solve the BTE is an hard task: recently deterministic solvers of the BTE, based of finite difference schemes, have been introduced [1] but their computational efforts is comparable to that of the Direct Simulation Monte Carlo.

Another alternative is to use Extended hydrodynamic models, based on the higher order moments of the BTE [2], but their sensitivity to the tail of the EED is an open question.

At the moment, the Monte Carlo (MC) solution of the BTE represents the most accurate approach for describing the tail of the EED, because the correct scattering mechanisms as well as the bands structure is taken into account. Unfortunately, the MC approach is CPU consuming, hence possibly unsuitable for extensive use in technology development. What we know from MC simulations is that the EED shape, for high energies, is maxwellian [3, 4] (for parabolic bands and acoustic and optical phonons scattering), whereas the electron-electron interaction modifies this asymptotic behaviour enhancing the tail [3, 5, 6].

The understanding of these phenomena has been the subject of a wide debate: according to some authors such tails reflect the distribution at the device boundaries due to ballistic transport [7, 8], or has been caused by 'superlucky' electrons which have absorbed more phonons than they have emitted [3].

A lot of effort has also been put into the development of analytical expression for the whole EED. Heuristic models for the EED are based on expansions around a global maxwellian [9], or polynomial in the exponential function [2, 10], or a combination of a global maxwellian and a power law of a global maxwellian (also known as 'stretched exponential') [11] in order to describe 'cold' and 'hot' electron populations. The parameters appearing in these EEDs can be determined by considering some approximation of the BTE and by fitting the resulting model to MC data.

The problem of the description of the high-energy tails has been tackled in a different context as in kinetic models for granular flows. A variety of analytical techniques have been developed such as by comparing the 'gain' and 'loss' terms in the BTE [12], or by means of a rigorous pointwise lower estimate [13], or by means of L^1 weighted tail control [14], or by using the so-called inelastic Maxwell models [15, 16].

The aim of this paper is to tackle the high-energy tail problem rigorously in the BTE framework, by using an analytical technique adapted from granular media which is based on moments estimate [14]. In this way, we are able to prove the existence of the EED tail which has the form of a 'stretched exponential'. The paper is organized as follows. In Section 2 the basic equations are written. In Section 3 the 'stretched exponential' for the tail is introduced and we formulate the main results. Section 4 is devoted to the moment inequalities. In Section 5 we present the proof of the main theorem. In Section 6 simulation results obtained by means of Direct Simulation Monte Carlo are shown and conclusion are drawn in Section 7.

2 Basic Equations

The Boltzmann transport equation (BTE) for one conduction band [17, 18] is

$$\frac{\partial f}{\partial t} + \mathbf{v}(\mathbf{k}) \cdot \nabla_{\mathbf{x}} f - \frac{q}{\hbar} \mathbf{E} \cdot \nabla_{\mathbf{k}} f = \mathcal{Q}[f] \quad , \quad (1)$$

where the unknown function $f(t, \mathbf{x}, \mathbf{k})$ represents the probability density of finding an electron at time t in the position $\mathbf{x} \equiv (x_1, x_2, x_3)$ with the wave-vector $\mathbf{k} \equiv (k_1, k_2, k_3)$,

and q is the absolute value of the electron charge. The domain of \mathbf{k} is the first Brillouin zone \mathcal{B} . In the neighborhood of the band minimum the dispersion relation can be considered approximately *quasi-parabolic*:

$$\varepsilon(\mathbf{k}) [1 + \alpha \varepsilon(\mathbf{k})] = \gamma = \frac{\hbar^2 \mathbf{k}^2}{2m^*}, \quad (2)$$

where m^* denotes the effective electron mass, which is $0.32 m_e$ (free electron mass) in silicon, α the non parabolicity factor (0.5 eV^{-1}), and \hbar the Planck constant divided by 2π . With this approximation the Brillouin zone \mathcal{B} coincides with \mathbb{R}^3 .

From eq.(2), the electron group velocity $\mathbf{v} \equiv (v_1, v_2, v_3)$ writes

$$\mathbf{v}(\mathbf{k}) = \frac{1}{\hbar} \nabla_{\mathbf{k}} \varepsilon = \frac{\hbar \mathbf{k}}{m^*} \frac{1}{\sqrt{1 + 4\alpha\gamma}}. \quad (3)$$

The parabolic band approximation is obtained from the previous equations with $\alpha=0$. The electric field $\mathbf{E}(t, \mathbf{x}) \equiv (E_1, E_2, E_3)$ satisfies the Poisson equation

$$\Delta(\epsilon\phi) = q [n(t, \mathbf{x}) - N_D(\mathbf{x}) + N_A(\mathbf{x})]$$

$$\mathbf{E} = -\nabla_{\mathbf{x}} \phi$$

where $\phi(t, \mathbf{x})$ is the electric potential, N_D and N_A , respectively, are the donor and acceptor densities, ϵ the dielectric constant, n the electron density given by

$$n(t, \mathbf{x}) = \int_{\mathbb{R}^3} f(t, \mathbf{x}, \mathbf{k}).$$

In general, for low electron density, the collision operator can be schematically written as

$$\mathcal{Q}[f] = \int_{\mathbb{R}^3} [w(\mathbf{k}', \mathbf{k}) f(\mathbf{k}') - w(\mathbf{k}, \mathbf{k}') f(\mathbf{k})] d\mathbf{k}' \quad (4)$$

where the first term represents the gain and the second one the loss, and $w(\mathbf{k}, \mathbf{k}')$ is the transition probability per unit time from a state \mathbf{k} to a state \mathbf{k}' .

The main scattering mechanisms in a silicon semiconductor are the electron-phonon interactions, the interaction with impurities, the electron-electron scatterings and the interaction with stationary imperfections of the crystal, as vacancies.

In this paper we shall consider electron-phonon interactions, and interaction with the impurities [18], i.e.

$$w(\mathbf{k}, \mathbf{k}') = w_{ac}(\mathbf{k}, \mathbf{k}') + w_{npo}(\mathbf{k}, \mathbf{k}') + w_{imp}(\mathbf{k}, \mathbf{k}'). \quad (5)$$

The first term represents the acoustic phonon scattering in the elastic approximation

$$\begin{aligned} w_{ac}(\mathbf{k}, \mathbf{k}') &= K_0 \delta(\varepsilon(\mathbf{k}') - \varepsilon(\mathbf{k})) \\ K_0 &= \frac{k_B T_L \Xi_d^2}{4 \pi^2 \hbar \rho v_s^2}, \end{aligned}$$

where T_L is the lattice temperature, Ξ_d the acoustic phonon deformation potential, ρ the silicon mass density and v_s the sound velocity of the longitudinal acoustic mode; the second term represents the non-polar optical scattering

$$w_{npo}(\mathbf{k}, \mathbf{k}') = K_1 [\mathbf{n}_q \delta(\varepsilon(\mathbf{k}') - \varepsilon(\mathbf{k}) - \hbar\omega) + (\mathbf{n}_q + 1) \delta(\varepsilon(\mathbf{k}') - \varepsilon(\mathbf{k}) + \hbar\omega)]$$

$$K_1 = \frac{(D_t K)^2}{8 \pi^2 \rho \omega}$$

where $\hbar\omega$ is the optical phonon energy and \mathbf{n}_q the phonon equilibrium distribution which, according to the Bose-Einstein statistics, is given by

$$\mathbf{n}_q = \frac{1}{\exp(\hbar\omega/k_B T_L) - 1} \quad .$$

The third and last term represents the ionized impurity scattering

$$w_{imp}(\mathbf{k}, \mathbf{k}') = \frac{K_2}{[\beta^2 + 2|\mathbf{k}|^2(1 - \cos \theta)]^2} \delta(\varepsilon(\mathbf{k}') - \varepsilon(\mathbf{k}))$$

$$K_2 = \frac{4Z^2 n_I q^4}{\hbar \kappa^2}$$

$$\cos \theta = \frac{\mathbf{k} \cdot \mathbf{k}'}{|\mathbf{k}| |\mathbf{k}'|}$$

The values of the coupling constants and the other parameters used for silicon are given in Table I.

The electron-electron interaction is taken into account in the framework of the mean field approximation through the Poisson equation. This is reasonable since we consider the case of low electron density and, therefore, we can neglect the short range collisions between electrons.

3 Exponential tails

In the following we shall draw our attention to the asymptotic behaviour of the steady state distribution function of the BTE

$$f_\infty(\mathbf{k}) = \lim_{t \rightarrow \infty} f(t, \mathbf{k})$$

for large $|\mathbf{k}|$, i.e. the high-energy tails. We expect that the behaviour of this solution is given by the so called 'stretched exponential', i.e.

$$f_\infty(\mathbf{k}) \simeq \exp[-r\varepsilon^s] \quad , \quad |\mathbf{k}| \rightarrow \infty \quad (6)$$

where r and s are some positive constants. We introduce the functionals [14]

$$\mathcal{F}_{r,s}(f) = \int_{\mathbb{R}^3} f(\mathbf{k}) \exp[r\varepsilon^s] d\mathbf{k} \quad (7)$$

and study the values of s and r for which these functionals are positive and finite. We can give the following definition:

Definition. We say that the function f has an *exponential tail of order* $s > 0$, if the following supremum

$$r_s^* = \sup\{r > 0 \mid \mathcal{F}_{r,s}(f) < +\infty\} \quad (8)$$

is positive and finite.

The functionals (7) can be represented by using the *symmetric moments* of the distribution function, i.e.

$$m_p = \int_{\mathbb{R}^3} f(\mathbf{k}) \varepsilon^p d\mathbf{k} \quad , \quad p \in \mathbb{R}_+ \quad . \quad (9)$$

In fact by expanding the exponential function in (7) into Taylor series we obtain (formally):

$$\mathcal{F}_{r,s}(f) = \int_{\mathbb{R}^3} f(\mathbf{k}) \left(\sum_{n=0}^{\infty} \frac{r^n}{n!} \varepsilon^{sn} \right) d\mathbf{k} = \sum_{n=0}^{\infty} \frac{m_{sn}}{n!} r^n \quad . \quad (10)$$

In order the expansion (10) have a sense, we shall suppose that the moments of all orders are finite. Then the value r_s^* can be interpreted as the **radius of convergence** of the series (10), and the order of the tail s is therefore the value for which the series has a positive and finite radius of convergence. For investigating the summability of the series (10) we look for estimates of the sequence of moments $\{m_p\}$, with $p = sn$, $n = 0, 1, 2, \dots$, and study the dependence of the estimate on $s > 0$. We shall be interested in the situation when the sequence of the coefficients satisfies

$$\frac{m_{sn}}{n!} \leq C Q^n, \quad n = 0, 1, 2, \dots \quad (11)$$

where C, Q are positive constants. In fact, according to the Hadamard theorem

$$\lim_{n \rightarrow \infty} \sqrt[n]{\frac{m_{sn}}{n!}} = \frac{1}{r_s^*}$$

and from the estimate (11) we have

$$r_s^* \geq \frac{1}{Q} > 0 \quad . \quad (12)$$

To achieve the estimate (11), we shall study the moments equations obtained by integrating against ε^p the BTE, in the **stationary and homogeneous** regime :

$$\mathcal{Q}_p + G_p = 0 \quad (13)$$

where

$$\mathcal{Q}_p = \int_{\mathbb{R}^3} \mathcal{Q}[f] \varepsilon^p d\mathbf{k} \quad (14)$$

$$G_p = \frac{q}{\hbar} \int_{\mathbb{R}^3} \mathbf{E} \cdot \nabla_{\mathbf{k}} f \varepsilon^p d\mathbf{k} \quad (15)$$

We underline that in the stationary and homogeneous regime, the electric field \mathbf{E} is a constant. Now we can formulate the main result of this paper:

Theorem 1. Let $f(\mathbf{k})$ be a nonnegative solution of the BTE (1) in the stationary and homogeneous regime, that has finite moments of all orders. Then the supremum r_s^* defined in (12) is finite for some $s > 0$, and in the energy range $\hbar\omega < \varepsilon < \varepsilon_0$, $\forall \varepsilon_0 > 0$.

To the best of our knowledge this is the first theorem which proves the existence of energy tails for the BTE in the semiconductor framework. This theorem proves also that the 'stretched exponential' (6), used in an heuristic way to model the EED tail, has a theoretical background. On the other hand, by using this technique, no information is given about the order of the tail s . This order will be determined by MC simulations in sec. 6. Our result is similar to that found in [14] for the BTE for granular media, where a shear flow model is considered as forcing term. But the scattering mechanism for granular flows is completely different respect to the semiconductor case, because binary inelastic collisions are considered between perfectly smooth hard sphere granular particles. The only analogy between the two cases, is the presence of an inelastic scattering mechanism in the collisional operator.

4 Moment inequalities

Let us introduce non dimensional variables:

$$\tilde{k} = \frac{k}{k_0}, \quad \tilde{v} = \frac{v}{v_0}, \quad \tilde{\varepsilon} = \frac{\varepsilon}{\varepsilon_0}, \quad \tilde{E} = \frac{E}{E_0}, \quad \tilde{\omega} = \frac{\hbar\omega}{\varepsilon_0}, \quad \tilde{\alpha} = \alpha k_B T_L$$

where

$$k_0 = \frac{\sqrt{m^* k_B T_L}}{\hbar}, \quad v_0 = \sqrt{\frac{k_B T_L}{m^*}}, \quad \varepsilon_0 = k_B T_L, \quad E_0 = \frac{k_B T_L \sqrt{m^* k_B T_L}}{q \hbar}$$

consequently by omitting the \sim , we can write

$$k^2 = 2\varepsilon(1 + \alpha\varepsilon), \quad \mathbf{v} = \frac{\mathbf{k}}{1 + 2\alpha\varepsilon}, \quad \varepsilon = \frac{-1 + \sqrt{1 + 2\alpha k^2}}{2\alpha}.$$

Now we change the variable \mathbf{k} into spherical coordinates, i.e.

$$\mathbf{k} \equiv (k_x, k_y, k_z) \longrightarrow (k \sin \theta \cos \phi, k \sin \theta \sin \phi, k \cos \theta) \quad (16)$$

and the density-of-state and the solid angle over the unit sphere are respectively:

$$J = (1 + 2\alpha\varepsilon) \sqrt{2\varepsilon(1 + \alpha\varepsilon)}, \quad d\sigma = \sin \theta d\theta d\phi.$$

The symmetric moments (9) write:

$$m_p = \int_{\mathbb{R}^3} f(\mathbf{k}) \varepsilon^p J d\varepsilon d\sigma. \quad (17)$$

Under suitable conditions on smoothness and decay for ε large of the solutions $f(\mathbf{k})$, the eq.(15) writes:

$$G_p = -p|\mathbf{E}| \int_{\mathbb{R}^3} f(\mathbf{k}) \varepsilon^p \frac{\mathbf{E} \cdot \mathbf{k}}{|\mathbf{E}||\mathbf{k}|} \frac{\sqrt{2\varepsilon(1+\alpha\varepsilon)}}{\varepsilon(1+2\alpha\varepsilon)} d\mathbf{k},$$

and from the definition of scalar product, and the eq.(17) we have the following bounds :

$$-2p|\mathbf{E}|m_{p-\frac{1}{2}} \leq G_p \leq 2p|\mathbf{E}|m_{p-\frac{1}{2}}. \quad (18)$$

Now we manipulate the term \mathcal{Q}_p (14):

$$\mathcal{Q}_p = \int_{\mathbb{R}^3} [w(\mathbf{k}', \mathbf{k})f(\mathbf{k}') - w(\mathbf{k}, \mathbf{k}')f(\mathbf{k})] \varepsilon^p d\mathbf{k}' d\mathbf{k} = \int_{\mathbb{R}^3} w(\mathbf{k}, \mathbf{k}')f(\mathbf{k}) [(\varepsilon')^p - \varepsilon^p] d\mathbf{k}' d\mathbf{k}$$

and from the scattering rate (5) we have:

$$\begin{aligned} \mathcal{Q}_p &= \mathcal{Q}_p^{(ac)} + \mathcal{Q}_p^{(npo)} + \mathcal{Q}_p^{(imp)} \\ \mathcal{Q}_p^{(ac)} &= K_0 \int_{\mathbb{R}^3} \delta(\varepsilon' - \varepsilon) f(\mathbf{k}) [(\varepsilon')^p - (\varepsilon)^p] d\mathbf{k}' d\mathbf{k} \\ \mathcal{Q}_p^{(npo)} &= K_1 \int_{\mathbb{R}^3} f(\mathbf{k}) [\mathbf{n}_q \delta(\varepsilon' - \varepsilon - \omega) + (\mathbf{n}_q + 1) \delta(\varepsilon' - \varepsilon + \omega)] [(\varepsilon')^p - (\varepsilon)^p] d\mathbf{k}' d\mathbf{k} \\ \mathcal{Q}_p^{(imp)} &= K_2 \int_{\mathbb{R}^3} \delta(\varepsilon' - \varepsilon) f(\mathbf{k}) [(\varepsilon')^p - (\varepsilon)^p] d\mathbf{k}' d\mathbf{k} \end{aligned}$$

The terms $\mathcal{Q}_p^{(el)}$ and $\mathcal{Q}_p^{(imp)}$ vanish due to the presence of $\delta(\varepsilon' - \varepsilon)$. By changing variables into spherical ones, after some manipulation, we have:

$$\mathcal{Q}_p = \mathcal{Q}_p^{(npo)} = \mathcal{Q}_p^{(+)} + \mathcal{Q}_p^{(-)}$$

where

$$\begin{aligned} \mathcal{Q}_p^{(+)} &= 4\pi 2^{\frac{1}{2}} \mathbf{n}_q K_1 \int_{\mathbb{R}^3} f(\mathbf{k}) [(\varepsilon + \omega)^p - \varepsilon^p] [1 + 2\alpha(\varepsilon + \omega)] \\ &\quad \times \sqrt{(\varepsilon + \omega) [1 + \alpha(\varepsilon + \omega)]} J d\varepsilon d\sigma \end{aligned} \quad (19)$$

$$\begin{aligned} \mathcal{Q}_p^{(-)} &= 4\pi 2^{\frac{1}{2}} (\mathbf{n}_q + 1) K_1 \int_{\mathbb{R}^3} f(\mathbf{k}) [(\varepsilon - \omega)^p - \varepsilon^p] [1 + 2\alpha(\varepsilon - \omega)] \\ &\quad \times \sqrt{(\varepsilon - \omega) [1 + \alpha(\varepsilon - \omega)]} \Theta(\varepsilon - \omega) J d\varepsilon d\sigma. \end{aligned} \quad (20)$$

Now we give an upper bound for $\mathcal{Q}_p^{(+)}$. By using the following inequalities

$$\begin{aligned} \sqrt{\varepsilon + \omega} &< \varepsilon + 2\omega \\ (\varepsilon + \omega)^p &\leq 2^{|p-1|} [\varepsilon^p + \omega^p] \quad , \forall p \geq 0 \end{aligned}$$

(where $\omega \simeq 2.4369$ in non dimensional units) and the definition (17), we obtain:

$$\begin{aligned} \mathcal{Q}_p^{(+)} \leq & 2^{\frac{3}{2}} \pi n_q K_1 2^{|p-1|} \left\{ \frac{\alpha^2}{2} m_{p+3} + \frac{1}{2} (3\alpha + 8\alpha^2 \omega) m_{p+2} + (10\alpha^2 \omega + 9\alpha \omega + 1) m_{p+1} \right. \\ & + 4\omega (2\alpha^2 \omega^2 + 3\alpha \omega + 1) m_p + 2^{p-1} \alpha^2 \omega^{p+1} m_3 + 2^{p-1} \omega^p (3\alpha + 8\alpha^2 \omega) m_2 \\ & \left. + (2\omega)^p (10\alpha^2 \omega^2 + 9\alpha \omega + 1) m_1 + \omega^{p+1} 2^{p+2} (2\alpha^2 \omega^2 + 3\alpha \omega + 1) m_0 \right\}. \quad (21) \end{aligned}$$

Now we give an upper bound for $\mathcal{Q}_p^{(-)}$. By using the inequalities:

$$\begin{aligned} \sqrt{\varepsilon - \omega} &> a(\varepsilon - \omega)^3, \text{ for } \omega < \varepsilon < \omega + \frac{1}{a^{\frac{2}{5}}} \quad \forall a > 0 \\ \varepsilon^p - (\varepsilon - \omega)^p &> \varepsilon^{p-1}, \text{ for } \varepsilon > \omega \quad \text{and} \quad p \geq \frac{1}{\omega} \simeq 0.41 \end{aligned}$$

we can write

$$[(\varepsilon - \omega)^p - \varepsilon^p] \sqrt{\varepsilon - \omega} < -\varepsilon^{p-1} a(\varepsilon - \omega)^3$$

and $\mathcal{Q}_p^{(-)}$ can be estimated as

$$\begin{aligned} \mathcal{Q}_p^{(-)} \leq & -4\pi 2^{\frac{1}{2}} (n_q + 1) K_1 a \int_{\mathbb{R}^3} f(\mathbf{k}) \varepsilon^{p-1} (\varepsilon - \omega)^3 [1 + 2\alpha(\varepsilon - \omega)] \\ & \times \sqrt{1 + \alpha(\varepsilon - \omega)} \Theta(\varepsilon - \omega) J d\varepsilon d\sigma. \end{aligned}$$

By using the further inequalities

$$\begin{aligned} \sqrt{1 + \alpha(\varepsilon - \omega)} &> \beta \varepsilon, \quad \text{with } \varepsilon < \frac{\alpha + \sqrt{\alpha^2 + 4\beta^2(1 - \alpha\omega)}}{2\beta^2}, \quad \forall \beta > 0 \\ 1 + 2\alpha(\varepsilon - \omega) &> \Gamma \varepsilon, \quad \text{with } \varepsilon < \frac{1 - 2\alpha\omega}{\Gamma - 2\alpha}, \quad \forall \Gamma > 2\alpha \end{aligned}$$

we obtain the final upper bound for $\mathcal{Q}_p^{(-)}$

$$\mathcal{Q}_p^{(-)} \leq -\pi (n_q + 1) K_1 a \beta \Gamma \left\{ 2^{-\frac{2}{3}} m_{p+4} - 3\omega 2^{-\frac{1}{2}} m_{p+3} + 3\omega^2 2^{\frac{1}{2}} m_{p+2} + \omega^3 2^{\frac{3}{2}} m_{p+1} \right\}. \quad (22)$$

Now we are ready to obtain a recursive inequality for the moments. From eq.(13) and the inequality (18), we get

$$-2p|E|m_{p-\frac{1}{2}} \leq \mathcal{Q}_p = \mathcal{Q}_p^+ + \mathcal{Q}_p^-$$

and using the upper bounds eqs.(21),(22), we obtain finally

$$\left\{ \begin{aligned} m_{p+1} &\leq R 2^{|p-4|} m_p + S_2 2^{|p-4|} m_{p-1} + S_1 2^{|p-4|} m_{p-2} + S_0 2^{|p-4|} m_{p-3} + T(p-3) m_{p-\frac{7}{2}} + \\ &V_3 2^{|p-4|} 2^{p-4} \omega^{p-2} m_3 + V_2 2^{|p-4|} 2^{p-4} \omega^{p-3} m_2 + V_1 2^{|p-4|} 2^{p-3} \omega^{p-3} m_1 + \\ &V_0 2^{|p-4|} 2^{p-1} \omega^{p-2} m_0 \\ &\forall p \geq 3 + \frac{1}{\omega} \simeq 3.4104, \quad \omega < \varepsilon < \varepsilon_M \end{aligned} \right. \quad (23)$$

where ε_M is an arbitrary fixed energy value, and the coefficients are positive constants given in the Appendix.

Assuming some properties of the moments of lower order, we can use the recursive inequality (23) to obtain information about the behaviour of the moments m_p , for p large.

5 Proof of theorem 1

We want to prove that the coefficients of the series (10) satisfy the inequality (11). First of all we show that **for every** $p \geq 1$ there exist C and Q positive constants, such that

$$m_p \leq CQ^p \quad . \quad (24)$$

To obtain the desired estimate, we split our proof in two parts

1. We fix p_0 and we prove that the inequality (24) holds for $1 \leq p \leq p_0$. We introduce the Jensen's inequality [19]:

Let be $\mathcal{C}[g(\mathbf{k})]$ a concave function and $f(\mathbf{k})$ a density probability, then

$$\int_{\mathbb{R}^3} f(\mathbf{k}) \mathcal{C}[g] d\mathbf{k} \leq \mathcal{C} \left[\int_{\mathbb{R}^3} f(\mathbf{k}) g(\mathbf{k}) d\mathbf{k} \right] . \quad (25)$$

For $1 \leq p \leq p_0$ we choose:

$$g(\mathbf{k}) = \varepsilon^{p_0}, \quad \mathcal{C}[g] = g^{\frac{p}{p_0}}$$

and from (25) we obtain

$$\int_{\mathbb{R}^3} f(\mathbf{k}) [\varepsilon^{p_0}]^{\frac{p}{p_0}} d\mathbf{k} \leq \left(\int_{\mathbb{R}^3} f(\mathbf{k}) \varepsilon^{p_0} d\mathbf{k} \right)^{\frac{p}{p_0}}$$

which can be written as:

$$\begin{cases} m_p \leq (m_{p_0})^{\frac{p}{p_0}} = CQ^p \\ 1 \leq p \leq p_0 \end{cases} \quad (26)$$

with $C=1$ and $Q=(m_{p_0})^{\frac{1}{p_0}}$.

2. We prove the inequality (24) for $p_0 < p < p_0 + 1$.

We can estimate the moments $m_{p_0-1}, m_{p_0-2}, m_{p_0-3}, m_{p_0-\frac{7}{2}}$ which appear in the

left-hand- side of (23) by using the inequality (26), supposing $p = p_0 \geq \frac{13}{2} + \frac{1}{\omega}$. The eq.(23) writes:

$$m_{p_0+1} \leq (2Q)^{p_0} \Gamma_1 + (4\omega)^{p_0} \Gamma_2 \quad (27)$$

where

$$\begin{cases} \Gamma_1 = \frac{1}{2^4} \left[R + S_2 Q^{-1} + S_1 Q^{-2} + S_0 Q^{-3} + 4T Q^{-\frac{7}{2}} \right] > 0 \\ \Gamma_2 = \frac{1}{2^8 \omega^2} V_3 m_3 + \frac{1}{2^8 \omega^3} V_2 m_2 + \frac{1}{2^7 \omega^2} V_1 m_1 + \frac{1}{2^5 \omega^2} V_0 m_0 > 0 \end{cases}$$

Now eq.(27) can be written as

$$m_{p_0+1} \leq \tilde{\Gamma} \tilde{Q}^{p_0} \quad (28)$$

where $\tilde{\Gamma} = 2 \max(\Gamma_1, \Gamma_2)$, and $\tilde{Q} = \max(2Q, 4\omega)$

By using induction arguments, from eq.(28) we can conclude that the inequality (24) holds for $p_0 < p < p_0 + 1$.

For every $p \geq 1$ we can cover the whole interval by using the previous arguments. A similar theorem is valid in the parabolic band approximation.

6 Simulation results

In the following we shall consider the bulk, where an homogeneous electric field is frozen into an homogeneous piece of silicon. The experimental evidence of the high-energy tails of the EED has been widely proved in literature by MC simulations. In the case of analytic parabolic band approximation (with acoustic and optical phonons scattering) this tail is a global maxwellian [3, 4]. So in principle we know, in this case, that the order of the tail in eq.(6) is $s = 1$. What is unknown is the radius of convergence r_s^* of the series (10), which is the inverse of the maxwellian temperature. This parameter will be determined by means of MC simulations.

Several fitting formula are given in literature for the whole EED in the quasi parabolic band approximation. Here we shall check the EED tail by means of eq.(6) determining, by using MC simulations, r_s^* and s in the quasi parabolic band approximations. An histogram of the numerical steady solution is obtained by changing variable from \mathbf{k} to $(\varepsilon, \theta, \phi)$ according to (16), discretizing the whole energy space in a system of concentric shells with increasing radius

$$\rho_n = n h, \quad n = 1, \dots, N, \quad h = \frac{R}{N}$$

and by counting the number of particles which are in the corresponding shells

$$\begin{aligned} f_1 &= \{\# \text{ particles} : \varepsilon < \rho_1\} \\ f_n &= \{\# \text{ particles} : \rho_{n-1} \leq \varepsilon < \rho_n\} \quad n = 2, \dots, N \\ f_{N+1} &= \{\# \text{ particles} : R \leq \varepsilon\} \quad . \end{aligned}$$

In order to obtain the parameters in (6), we rewrite this equation into the form:

$$f_n = c \exp \left[- \left(\frac{\varepsilon_n - \varepsilon_{n_0}}{T_M} \right)^s \right] , n \geq n_0$$

and plot the pairs (x_n, y_n)

$$x_n = \ln(\varepsilon_n - \varepsilon_{n_0}) , y_n = \ln(\ln f_{n_0} - \ln f_n) , n = n_0 + 1, \dots, N .$$

Thus we expect that

$$y_n = s x_n + b \tag{29}$$

where

$$b = -s \ln T_M \tag{30}$$

is an almost linear plot for large values of the energy, whose slope is the exponent s , and the y-intercept is related to the parameter T_M (whose dimension is an energy). In figure 1 we show the simulation results obtained in the parabolic band approximation (i.e. $\alpha=0$ in eqs.(2),(3)) with an electric field of 80 KV/cm. The solid curve shows the MC data y_n , while the dashed straight line represents eq.(29) with $s=1$ and $T_M = 4907$ K. Thus the asymptotic EED is the global maxwellian

$$f_\infty \simeq \exp \left[- \frac{\varepsilon}{T_M} \right] .$$

In figure 2 we show the slope s as function of the electric field, both for parabolic and quasi parabolic band approximations. In the parabolic band approximation this value is approximately one (i.e. the EED has a global maxwellian tail), but in the quasi parabolic case the EED tail is given by the 'stretched exponential' (6). The parameter s is a function of the electric field, and for small field values, approaches the value one, i.e. the tail is a global maxwellian.

In figure 3 we show the parameter T_M as function of the electric field, both for parabolic and quasi parabolic band approximations. For moderate values of the electric field this parameter coincides with the lattice temperature (dashed straight line), but for higher values this parameter increases. This behaviour can be justified as follows: r_s^* is the convergence radius of the power series (10), which is subject to the inequality (12), where Q is a function of the electric field E .

7 Conclusions

In this paper we have proved the existence of high-energy tails for the EED of the BTE (in the analytic band approximations, and scattering with acoustic and optical phonon and impurities), with a moment inequality technique, adapted from the granular flows [14]. We have also proved that the 'stretched exponential' (6), used in an heuristic way to model the EED tail, has a theoretical background. Our theoretical results are

confirmed by MC simulations for bulk silicon. In particular, in the parabolic band approximation, the tail is a global maxwellian whose temperature coincides with the lattice temperature for moderate electric fields whereas, for higher values, this temperature increases. In the quasi parabolic case the tail is a 'stretched exponential' (6). In the future we shall try to extent the same technique to other scattering mechanisms, such as electron-electron. Another line of research will be to use other analytic techniques in order to obtain exact information about the order s of the tail.

Acknowledgments

This work has been supported by MIUR PRIN 2004 "Modelli per il trasporto di cariche nei semiconduttori: aspetti analitici e computazionali", "Progetti di ricerca di Ateneo" Università degli Studi di Catania, EU Marie Curie RTN project COMSON grant n. MRNT-CT-2005-019417 .

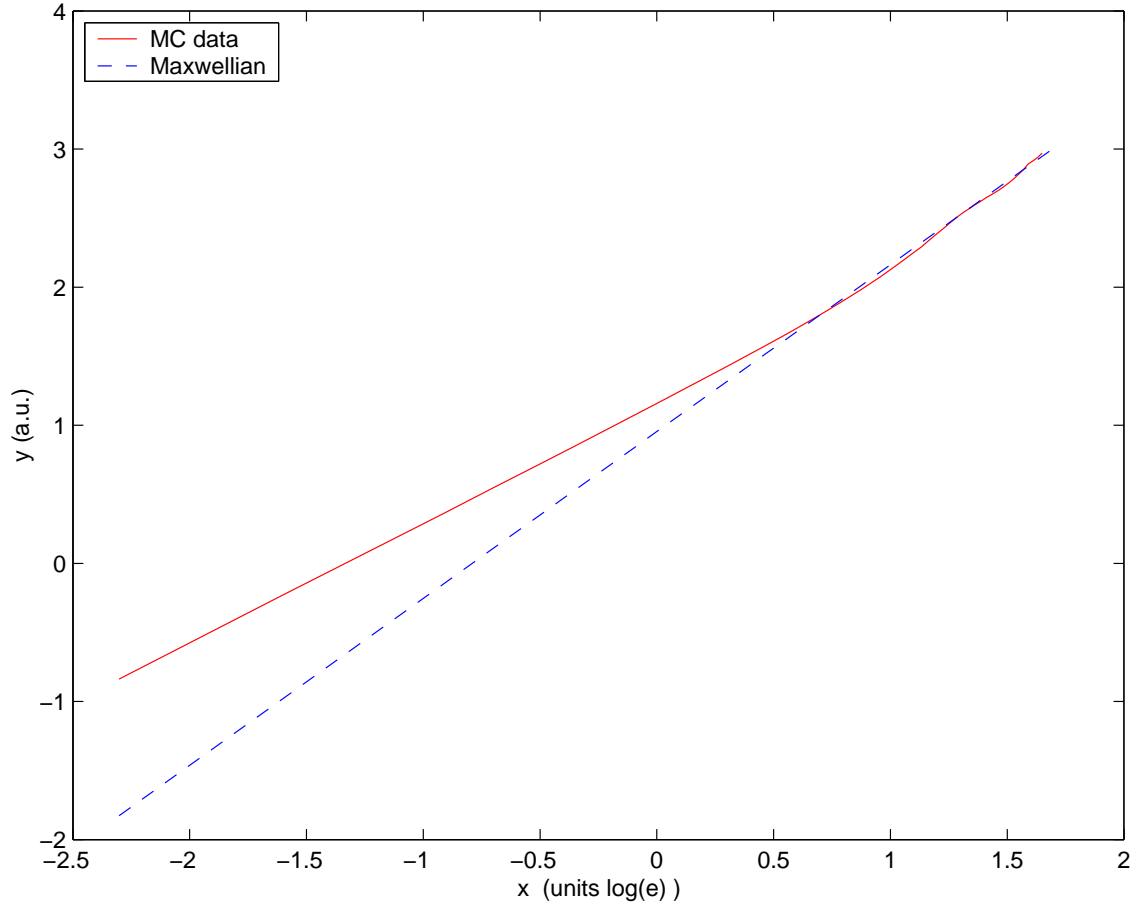


Figure 1: Logarithmic plot of the EED obtained with MC simulation (solid curve) and with eq.(29) (solid dashed straight line) with $s=1$ and $T_M = 4907$ K. The electric field is 80 KV/cm and the parabolic band approximation is used.

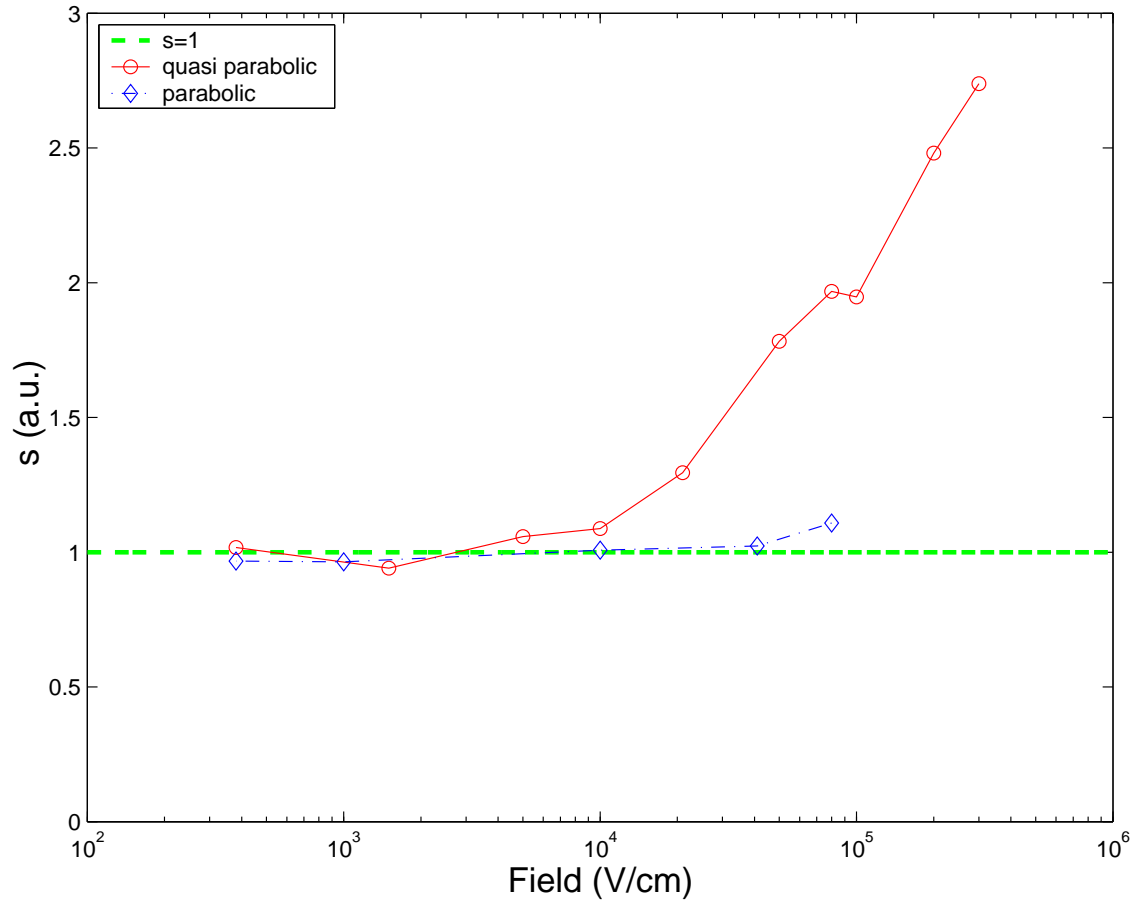


Figure 2: The parameter s as function of the electric field, for parabolic and quasi parabolic band approximations. The dashed straight line ($s=1$) indicates a global Maxwellian tail.

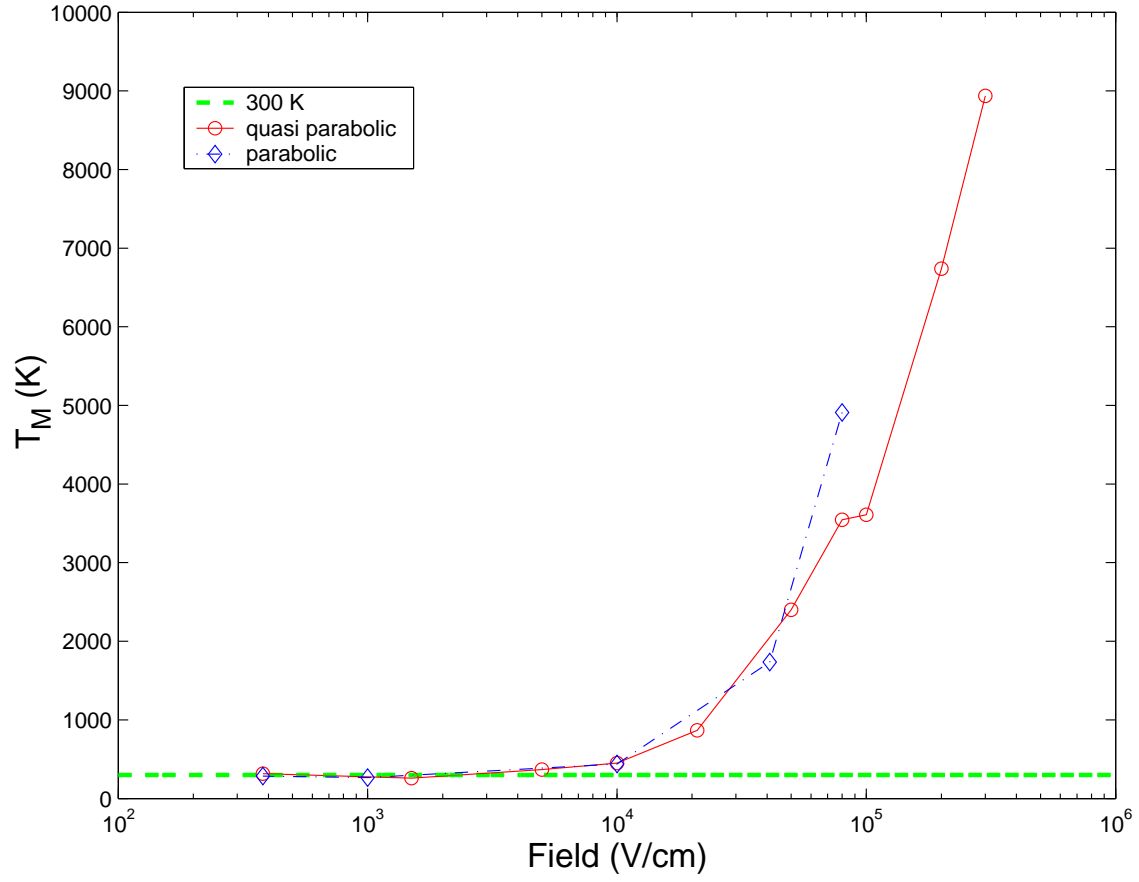


Figure 3: The parameter T_M as function of the electric field, for parabolic and quasi parabolic band approximations. The dashed straight line indicates the lattice temperature 300⁰ K .

References

- [1] J. Carrillo, I. Gamba, A. Majorana and C.-W. Shu, "A WENO-solver for 1d non-stationary Boltzmann-Poisson system for semiconductor devices", Jour. Comp. Electronics, **1**, 365-370, (2002)
- [2] Anile A.M. and Romano V. : Nonparabolic band transport in semiconductors: closure of the moment equations, Cont. Mech. Therm., **11**, 307-325, (1999)
- [3] A. Abramo, C. Fiegna, J. Appl. Phys. **80** , 889–893, (1996)
- [4] C.C.C. Leung, P.A. Childs, Appl. Phys. Lett., **66**(2), 162–164, (1995)
- [5] M.V. Fischetti, S.E. Laux, IEDM Tech. Dig., 305–308 , (1995)
- [6] J.E. Chung, M.-C. Jeng, J.E. Moon, P.-K. Ko, and C .Hu, IEEE Tran. Elec. Dev., **ED-37**, 1651, (1990)
- [7] A. Lacaita, Appl. Phys. Lett., **59** , 1623, (1991)
- [8] M. Mastrapasqua, J. Bude, Microelec. eng, **28** , 293, (1995)
- [9] Struchtrup H. , Physica A , **275**, 229, (2000)
- [10] Cassi D. and Ricco' B.: An analytical model of the energy distribution of hot electrons, IEEE Trans. elec. dev. , **37**, 1514–1521, (1990)
- [11] Grasser T., Kosina H., Heitzinger C. and Selberherr S.: Characterization of the hot electron distribution function using six moments, J. Appl. Phys., **91**, 3869–3879, (2002)
- [12] M.H. Ernst, R. Brito : Driven inelastic models with high energy tails, Phys. Rev. E, **65**,040301(1-4), (2002)
- [13] I.M. Gamba, V. Panferov and C. Villani : On the Boltzmann equation for diffusively excited granular media, Comm. Math. Phys., **246**,503-541,(2004)
- [14] A.V. Bobylev, I.M. Gamba, V. Panferov : Moment inequalities and high-energy tails for Boltzmann equations with inelastic interactions, J. Stat. Phys. **116**, 1651-1682 , (2004)
- [15] A.V. Bobylev, J.A. Carrillo, I.M. Gamba, : On some properties of kinetic and hydrodynamic equations for inelastic interactions, J. Stat. Phys., **98**, 743-773,(2000)
- [16] A.V. Bobylev, C. Cercignani: Moment equations for a granular material in a thermal bath, J. Stat. Phys., **106**, 547-567,(2002)
- [17] Markowich A. , Ringhofer C.A. and Schmeiser C., *Semiconductor equations* , Springer-Verlag, Wien, (1990)

- [18] Jacoboni C. and Reggiani L.: The Monte Carlo method for the solution of charge transport in semiconductors with applications to covalent materials , Rev. Mod. Phys., **55** , 645–705, (1983)
- [19] C. Cercignani, *The Boltzmann equation and its applications*, Springer, New York (NY), 1988

Table I. Silicon parameters

m_e	electron rest mass	9.109510^{-28} g
m^*	effective mass	$0.32 m_e$
T_L	lattice temperature	300 $^{\circ}K$
ρ_0	density	2.33 g/cm ³
v_s	longitudinal sound speed	$9.18 \cdot 10^5$ cm/sec
Ξ_d	acoustic phonon deformation potential	9 eV
$\hbar\omega$	optical phonon energy	63 meV
$D_t K$	optical phonon deformation potential	$11 \cdot 10^8$ eV/cm

Appendix

$$R = \frac{2\chi}{a\Gamma\beta} \frac{n_q}{n_q + 1}, T = \frac{2^{\frac{5}{2}}|E|}{\pi(n_q + 1)Ba\Gamma\beta}, S_2 = \frac{2^2}{a\Gamma\beta} \frac{n_q}{n_q + 1} (3\alpha + 8\alpha^2\omega)$$

$$S_1 = \frac{2^3}{a\Gamma\beta} \frac{n_q}{n_q + 1} (10\alpha^2\omega + 9\alpha\omega + 1), S_0 = \frac{2^5}{a\Gamma\beta} \frac{n_q}{n_q + 1} \omega (2\alpha^2\omega^2 + 3\alpha\omega + 1)$$

$$V_3 = \frac{2^3}{a\Gamma\beta} \frac{n_q}{n_q + 1} \alpha^2, V_2 = \frac{2^3}{a\Gamma\beta} \frac{n_q}{n_q + 1} (8\alpha^2\omega + 3\alpha),$$

$$V_1 = \frac{2^3}{a\Gamma\beta} \frac{n_q}{n_q + 1} (10\alpha^2\omega^2 + 9\alpha\omega + 1), V_0 = \frac{2^3}{a\Gamma\beta} \frac{n_q}{n_q + 1} (2\alpha\omega^2 + 3\alpha\omega + 1)$$

where $\chi = 2\alpha^2 + M\Gamma\beta a$, and $M \in [0, 168]$.